THE JOURNAL OF BIOLOGICAL CHEMISTRY VOL. 287, NO. 39, pp. 32981–32992, September 21, 2012

Integrin $\alpha_2\beta_1$ Mediates Tyrosine Phosphorylation of Vascular Endothelial Cadherin Induced by Invasive Breast Cancer Cells*

Received for publication, June 27, 2012, and in revised form, July 24, 2012 Published, JBC Papers in Press, July 25, 2012, DOI 10.1074/jbc.M112.395905

Mehran Haidari[‡§1], Wei Zhang[§], Amy Caivano[§], Zhenping Chen[§], Leila Ganjehei[§], Ahmadreza Mortazavi[§], Christopher Stroud[‡], Darren G. Woodside[§], James T. Willerson[‡§], and Richard A. F. Dixon[§]

From the [‡]Department of Internal Medicine, Division of Cardiology, University of Texas Medical School at Houston, Houston, Texas 77030 and the [§]Texas Heart Institute at St. Luke's Episcopal Hospital, Houston, Texas 77030

Background: The disruption of endothelial barrier function by tumor cells was studied.
Results: The attachment of tumor cells to endothelial cells leads to the disorganization of endothelial adherens junction.
Conclusion: Interaction of tumor cells with endothelial cells alters endothelial signaling and facilitates cancer cell diapedesis.
Significance: This study introduces new therapeutic targets for treating metastatic breast cancer.

The molecular mechanisms that regulate the endothelial response during transendothelial migration (TEM) of invasive cancer cells remain elusive. Tyrosine phosphorylation of vascular endothelial cadherin (VE-cad) has been implicated in the disruption of endothelial cell adherens junctions and in the diapedesis of metastatic cancer cells. We sought to determine the signaling mechanisms underlying the disruption of endothelial adherens junctions after the attachment of invasive breast cancer cells. Attachment of invasive breast cancer cells (MDA-MB-231) to human umbilical vein endothelial cells induced tyrosine phosphorylation of VE-cad, dissociation of β-catenin from VE-cad, and retraction of endothelial cells. Breast cancer cell-induced tyrosine phosphorylation of VE-cad was mediated by activation of the H-Ras/Raf/MEK/ERK signaling cascade and depended on the phosphorylation of endothelial myosin light chain (MLC). The inhibition of H-Ras or MLC in endothelial cells inhibited TEM of MDA-MB-231 cells. VE-cad tyrosine phosphorylation in endothelial cells induced by the attachment of MDA-MB-231 cells was mediated by MDA-MB-231 $\alpha_2\beta_1$ integrin. Compared with highly invasive MDA-MB-231 breast cancer cells, weakly invasive MCF-7 breast cancer cells expressed lower levels of $\alpha_2\beta_1$ integrin. TEM of MCF-7 as well as induction of VE-cad tyrosine phosphorylation and dissociation of β-catenin from the VE-cad complex by MCF-7 cells were lower than in MDA-MB-231 cells. These processes were restored when MCF-7 cells were treated with β_1-activating antibody. Moreover, the response of endothelial cells to the attachment of prostatic (PC-3) and ovarian (SKOV3) invasive cancer cells resembled the response to MDA-MB-231 cells. Our study showed that the MDA-MB-231 cell-induced disruption of endothelial adherens junction integrity is triggered by MDA-MB-231 cell $\alpha_2\beta_1$ integrin and is mediated by H-Ras/MLC-induced tyrosine phosphorylation of VE-cad.

Tumor cell migration depends on the invasive capacity of tumor cells and their ability to breach the endothelial cell barrier. During the process of hematogenous metastasis, circulating tumor cells must overcome the endothelial barrier to extravasate. However, the precise molecular mechanism of tumor cell extravasation has been poorly defined. A widely supported model is that the adhesion of tumor cells to the endothelium or the secretion of growth factors by cancer cells disrupts the integrity of endothelial barrier function. The integrity of the vascular endothelium is primarily dependent upon the organization of interendothelial adherens junctions. These junctions are formed by the homotypic interaction of vascular endothelial cadherin (VE-cad),[2] which is a transmembrane protein that forms a complex with an intracellular protein network, including α-, β-, and γ-catenin. VE-cad is found specifically in endothelial cell adherens junctions and may play fundamental roles in controlling transport across the endothelial barrier and in regulating angiogenesis (1, 2).

To maintain endothelial barrier function, VE-cad activity is tightly regulated through mechanisms that involve protein phosphorylation and cytoskeletal dynamics. Phosphorylation of VE-cad on Tyr residues disrupts endothelial cell adherens junctions by causing the dissociation of catenins from VE-cad, facilitating the diapedesis of leukocytes and metastatic cancer cells (3–5). Previously, the endothelium has been shown to act as a protective barrier against the invasion of cancer cells and, hence, metastasis (6). Transmigrating tumor cells are thought to overcome the endothelial barrier by inducing changes in endothelial cells, including the reorganization of the cytoskeleton (7), Src-mediated disruption of endothelial VE-cad·β-catenin complexes (5), the formation of gaps between endothelial cells (8), and the induction of apoptosis (9). However, the validity of this paradigm has recently been called into question. Endothelial cells have been shown to modulate the invasiveness of several types of cancer cells by increasing their dissemination

* This work was supported by MacDonald General Research Fund Grant 09RDM002 (to M. H.).
[1] To whom correspondence should be addressed: Texas Heart Institute at St. Luke's Episcopal Hospital, P.O. Box 20345, C1000, Houston, TX 77030. Tel.: 832-355-9077; Fax: 832-355-9333; E-mail: Mehran.Haidari@uth.tmc.edu.

[2] The abbreviations used are: VE-cad, vascular endothelial cadherin; HUVEC, human umbilical vein endothelial cell; MLC, myosin light chain; TEM, transendothelial migration; DN, dominant negative.

through vessels (10) or by increasing their invasive capability to migrate into the extracellular matrix (11, 12). Most previous studies regarding the molecular mechanisms underlying tumor cell metastasis have focused on the role of cancer cells, whereas the mechanisms that protect endothelial barrier integrity during the diapedesis of metastatic cancer cells remain elusive. In our study, we explored the molecular pathways that regulate the disruption of endothelial barrier function after the attachment of invasive breast cancer cells. Tumor cell invasion may closely resemble leukocyte trafficking, in which the endothelium acts as a barrier and greatly reduces invasion rates (13). Recently, we identified signal transduction pathways that regulate the transendothelial migration (TEM) of monocytes (14). In the present study, we determined that the attachment of invasive breast cancer cells (MDA-MB-231 cells) to endothelial cells leads to the disorganization of adherens junction structure and Tyr phosphorylation of VE-cad. Furthermore, we characterized the mechanisms underlying these events by identifying roles for $\alpha_2\beta_1$ integrin, endothelial H-Ras/Raf/MEK/ERK signaling, and myosin light chain (MLC) phosphorylation.

EXPERIMENTAL PROCEDURES

Reagents—Phospho-specific and nonphospho-specific antibodies against Src (Tyr(P)-416), Pyk2 (Tyr(P)-402), β-catenin, and ERK1/2 were purchased from Abcam (Cambridge, MA). Phospho-specific antibodies and nonphospho-specific antibodies against VE-cadherin (Tyr-731) were purchased from Invitrogen. Monoclonal β_1 integrin-activating TS2/16 was from American Type Culture Collection (Manassas, VA). β_1 integrin-blocking mAb (33B6) was a generous gift from Dr. Bradley McIntyre (University of Texas MD Anderson Cancer Center, Houston, TX). Monoclonal phospho-antibody against MLC and specific antibody against MLC were purchased from Sigma-Aldrich. Monoclonal antibodies against α_{1-3}, α_9, β_{1-3}, and $\alpha_v\beta_3$ were purchased from Millipore (Temecula, CA). Monoclonal antibodies against α_5 and rat IgG were purchased from BD Biosciences. Monoclonal antibodies against α_4 and α_6 were purchased from ABD Serotec (Raleigh, NC). Monoclonal antibody against β_7 was purchased from Santa Cruz Biotechnology, Inc. (Santa Cruz, CA). Mouse IgG was purchased from Southern Biotech (Birmingham, AL). Recombinant IL-1, monocyte chemoattractant protein, and cytochalasin D were purchased from Calbiochem. Recombinant human $\alpha_2\beta_1$, $\alpha_3\beta_1$, and $\alpha_5\beta_1$ were purchased from R&D Systems (Minneapolis, MN). Premade recombinant Ras N17 (dominant negative (DN)), RhoA N19 (DN), Raf-1 (DN), ERK2 (DN), Cdc42 N17 (DN), RAC1 N17, null control and GFP adenoviruses, and ViraDuctin adenovirus transduction reagents were purchased from Cell Biolabs, Inc. (San Diego, CA). The mutant construct for MLC, in which Thr-18 and Ser-19 were replaced with alanines (A-A-MLC) so that the protein could not be phosphorylated, was a generous gift from Dr. Andreas Kapus (University of Toronto) (15). siRNA and TaqMan primers and probes for Src, Pyk2 (PTK2B), β_1, β_2, $\alpha_v\beta_3$, and α_{2-6} integrin subunits were purchased from Applied Biosystems (Foster City, CA).

Cells—Human umbilical vein endothelial cells (HUVECs), human breast cancer cells (MDA-MB-231 and MCF-7), and human ovarian and prostatic cancer cells (PC-3) were purchased from ATCC. HUVECs were grown in Lonza EGM-2-MV medium on collagen-coated (20 μg/ml) tissue culture dishes. HUVECs from fewer than 4 generations were used for all experiments. The cancer cells were maintained in DMEM medium with 10% heat-inactivated FCS.

Interaction of Cancer Cells with Endothelial Cells—Tumor cells were detached from a 75-mm flask by trypsin and were then added to a monolayer of HUVECs (3×10^6 cancer cells/1×10^6 HUVECs). There was a firm adhesion of cancer cells to HUVECs 10 min after the addition (the cancer cells were not detached from HUVECs after vigorously washing with PBS). To avoid the contamination of HUVEC lysates with cancer cells, the maximum time allowed for the interaction of cancer cells with HUVECs was 7 min.

Western Blotting—HUVECs were grown to confluence in 35-mmol/liter dishes or 6-well plates. Cells were extracted in radioimmunoprecipitation assay buffer, which contained 0.1% SDS, 1% deoxycholate, 1% Nonidet P-40, 10 mmol/liter sodium phosphate, 150 mmol/liter NaCl, 2 mmol/liter EDTA, 50 mmol/liter NaF, 5 mmol/liter sodium pyrophosphate, 0.1 mmol/liter sodium vanadate, 2 mmol/liter PMSF, 0.1 mg/ml leupeptin, and 100 KIU/ml aprotinin. Samples were loaded onto an SDS-polyacrylamide gel and run at 150 V for 1 h. The proteins were then transferred onto nitrocellulose paper at 300 mA for 1.5 h, followed by Western blot analysis. Blots were blocked with 5% dry milk in 0.1% Tween 20 in PBS for 1 h at room temperature. The primary antibodies were used at a dilution of 1:500 to 1:1000. All antibodies were added for 1 h at room temperature or overnight at 4 °C. After washing, the appropriate secondary antibodies (Pierce) were added at a dilution of 1:10,000 for 1 h at room temperature. After extensive washing, blots were developed with the SuperSignal enhanced chemiluminescence kit (Pierce) and visualized on Kodak-AR film.

Immunoprecipitation—Cells were grown to confluence, washed gently with ice-cold PBS twice, and lysed in 1 ml of radioimmunoprecipitation assay lysis buffer. After 10 min on ice, cell lysates were collected and precleared for 30 min at 4 °C with protein A-agarose. After centrifugation (14,000 × *g*, 15 s at 4 °C), the supernatants were incubated with primary antibodies (1 μg/mg lysate) overnight at 4 °C with continuous mixing. Protein A-agarose (40 μl) was added to the lysate. After 2 h at 4 °C, the beads were washed three times in lysis buffer, and proteins were eluted by boiling in SDS-sample buffer containing 4% 2-mercaptoethanol (Bio-Rad). The samples were analyzed by SDS-PAGE.

Cell Adhesion Assay—HUVECs were seeded into 24-well plates and grown to confluence. Tumor cells (25×10^6) were resuspended in 1 ml of complete medium and incubated for 1 h at 37 °C in the presence of 50 μg/ml calcein-AM (Molecular Probes, Invitrogen). After the cells were labeled, they were resuspended at a concentration of 1×10^6 cells/ml in DMEM. Tumor cells (1.5×10^5 in 150 μl) were added to washed plates and incubated for 30 min at 37 °C. After incubation, plates were washed three times with DMEM. Adherent cells were lysed, and cell adhesion was quantified on an Ultra384 plate reader (Tecan, Männedorf, Switzerland) by using 485- and 535-nm excitation and emission filters, respectively, after cell lysis in

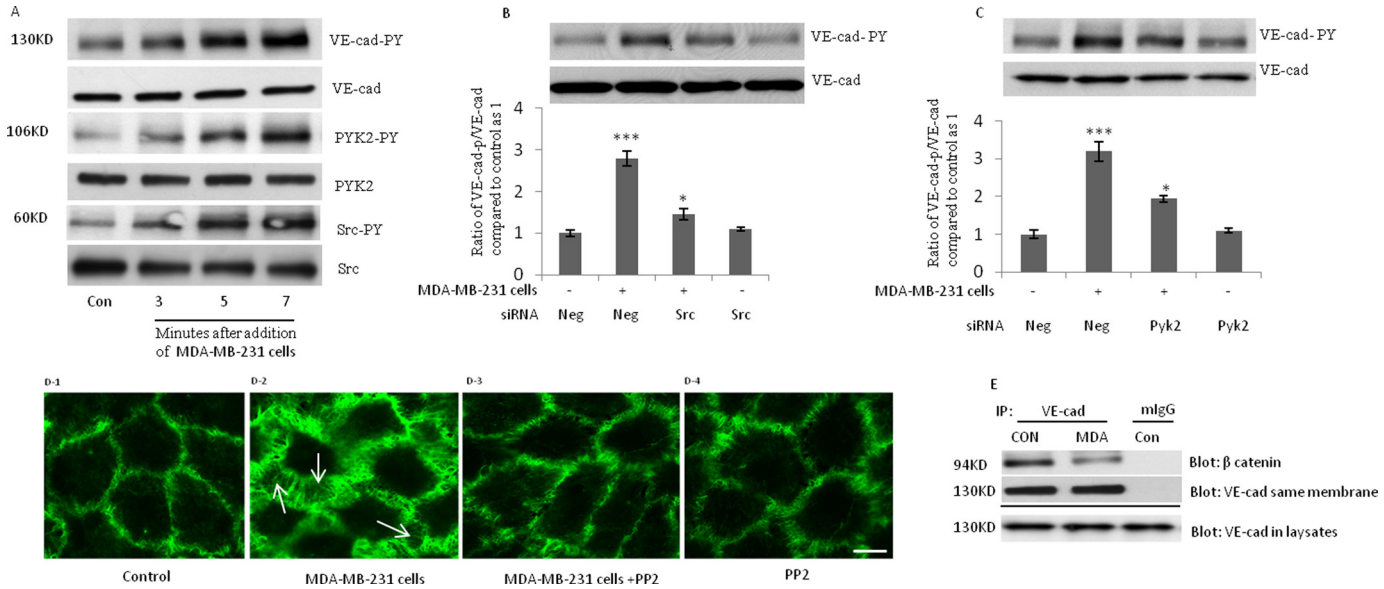

FIGURE 1. **Attachment of MDA-MB-231 cells to HUVECs induces Tyr phosphorylation of VE-cad, dissociates β-catenin from VE-cad, and retracts endothelial cells.** *A*, Tyr phosphorylation of VE-cad, Src, and Pyk2 was induced in HUVECs after the addition of MDA-MB-231 cells (3×10^6 MDA-MB-231 cells/1×10^6 HUVECs). *B* and *C*, MDA-MB-231 cell-induced VE-cad Tyr phosphorylation depended on Src and Pyk2. HUVECs were transfected with the indicated siRNA and were exposed to MDA-MB-231 cells for 5 min (3×10^6 of MDA-MB-231 cells/1×10^6 HUVECs). *Neg*, scrambled siRNA control. *D*, attachment of MDA-MB-231 cells to HUVECs led to the retraction of HUVECs. MDA-MB-231 cells were trypsinized, washed, and added to HUVECs for 10 min. Cells were fixed with 4% paraformaldehyde and stained with primary rabbit polyclonal antibody against VE-cad and secondary FITC-conjugated goat anti-rabbit IgG antibody (*green*). *D1*, control HUVECs without the addition of MDA-MB-231 cells. *D2*, retraction of HUVECs 10 min after the addition of MDA-MB-231 cells (3×10^6 MDA-MB-231 cells/1×10^6 HUVECs). *D3*, retraction of HUVECs inhibited by the pretreatment of HUVECs with PP2 (10 μM, 2h) before the addition of MDA-MB-231 cells. *D4*, HUVECs treated with PP2 (10 μM, 2 h). *White arrow*, gaps formed between HUVECs. *Bar*, 10 μm. *E*, attachment of MDA-MB-231 cells to HUVECs led to the dissociation of β-catenin from VE-cad. MDA-MB-231 cells (3×10^6 MDA-MB-231 cells/1×10^6 HUVECs) were added to HUVECs, and after 5 min, HUVECs were washed and used for the immunoprecipitation assay. MDA, MDA-MB-231 cells. *, $p < 0.05$; ***, $p < 0.001$, *versus* control. Each experiment was independently performed 3–4 times. *Error bars*, S.E.

lysis buffer containing 50 mmol/liter Tris-HCl (pH 7.5), 1% Nonidet P-40, and 5 mmol/liter EDTA.

Pull-down Assay for H-Ras—Pull-down assays for Ras were performed according to the manufacturer's instructions (Pierce). HUVECs were lysed in lysis buffer (25 mmol/liter Tris-HCl, pH 7.5, 150 mmol/liter NaCl, 5 mmol/liter $MgCl_2$, 1% Nonidet P-40, 1 mmol/liter DTT, and 5% glycerol) on ice for 5 min. The lysates were centrifuged at 16 000 × *g* at 4 °C for 15 min. Activated Ras was pulled down with GST·Raf1·Ras-binding domain complex followed by Western blotting for active Ras.

Flow Cytometry—Tumor cells were trypsinized and resuspended in 100 μl of FACS buffer (1×10^6 cells/tube). The cells were treated with 1 μg of antibody and were incubated on ice for 1 h. The cells were washed, secondary FITC antibody was added, and cells were incubated for 30 min on ice. The cells were then washed with cold FACS buffer, resuspended in 400 μl of FACS buffer, and used for analysis. Fluorochrome- and isotype-matched controls were used in parallel experiments to monitor nonspecific staining. All data were recorded with a BD FACS LSRII and analyzed with FlowJo 7.6.1.

Transduction of Adenovirus—The conditions used for the transduction of recombinant adenoviruses were optimized by using adenovirus encoding GFP. All reagents and kits, including transduction reagents, an adenovirus purification kit, and an adenovirus titration kit, were purchased from Cell Biolabs, Inc. After purification, the titration of each recombinant adenovirus was determined by an ELISA titrating kit. HUVECs were seeded into 6-well plates for 24 h until they reached 80% confluence. According to the manufacturer's protocol, adenovirus was transduced into cells by using ViraDuctin (Cell Biolabs, Inc.). HUVECs were infected with adenoviral vectors with a multiplicity of infection of 100 plaque-forming units/cell in the presence of ViraDuctin. After incubation with viral particles for 48 h, the cells were assessed for the expression of the transduced genes. The efficacy of all recombinant adenoviruses was previously tested (14).

Transfection of siRNA and Plasmids—An FITC-labeled, double-stranded siRNA (Invitrogen) was used to optimize the transfection of endothelial cells with siRNA. The siRNA constructs for Src Pyk2, β_1, and α_{2-6} were validated by Applied Biosystems (Foster City, CA). To confirm the efficiency of siRNA transfection, the mRNA expression of genes of interest was measured by RT-PCR (15), and protein expression was analyzed by flow cytometry. The vector pcDNA3.1/CT-GFP TOPO (Invitrogen) was used to optimize the transfection of plasmids into HUVECs. Plasmids and siRNA were transfected into cells by using Lipofectamine 2000 (Invitrogen). Scrambled siRNA (a non-targeting siRNA pool) and empty pcDNA3.1 vector were transfected as controls. Cells were collected 48 h after transfection with siRNA or plasmids.

Immunofluorescence Studies—Cells were grown in wells of 4-chamber culture collagen-coated slides. Cells were fixed in 4% paraformaldehyde for 15 min at 4 °C, washed with PBS, and permeabilized for 5 min with 0.1% Triton X-100. After blocking with PBS plus 2% BSA plus 0.1% Tween 20, cells were incubated with primary antibody against VE-cad and goat anti-rabbit IgG for 45 min each. Images were acquired by MicroSuite FIVE

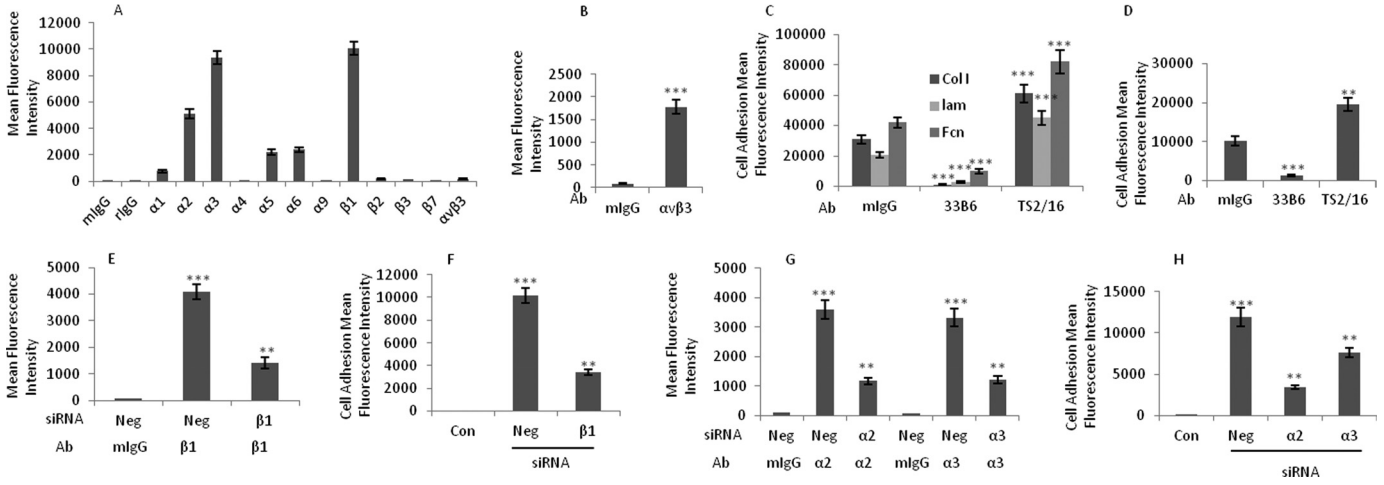

FIGURE 2. **Adhesion of MDA-MB-231 cells to HUVECs is dependent on the expression of β_1 integrins on MDA-MB-231 cells.** *A*, flow cytometry analysis shows the expression of α and β integrin subunits on MDA-MB-231 cells. *mIgG*, mouse IgG; *rIgG*, rat IgG. *B*, flow cytometry analysis shows the expression of $\alpha_v\beta_3$ integrin on HUVECs. *C*, β_1 integrin-blocking antibody and β_1 integrin-activating antibody inhibited and enhanced, respectively, the attachment of MDA-MB-231 cells to laminin, fibronectin, and collagen type I. The 96-well plates were coated with laminin (3 μg/ml), fibronectin (5 μg/ml), or collagen type I (0.2 μg/ml) before the adhesion assay was performed. MDA-MB-231 cells were treated with 1 μg/ml β_1 integrin-blocking antibody (33B6), β_1 integrin-activating antibody (TS2/16), or mouse IgG for 1 h and were then used for the adhesion assay. *D*, attachment of MDA-MB-231 cells to HUVECs was inhibited by a β_1 integrin-blocking antibody and enhanced by a β_1 integrin-activating antibody. MDA-MB-231 cells were treated with the β_1 integrin-blocking antibody (33B6; 1 μg/ml) or a β_1 integrin-activating antibody (TS2/16; 1 μg/ml) for 1 h, washed, and subjected to the adhesion assay. *E*, flow cytometry analysis shows that the expression of β_1 integrins on MDA-MB-231 cells was inhibited after treatment with siRNA against the β_1 integrin subunit. Scrambled siRNA (*Neg*) was used as a control. *F*, treatment of MDA-MB-231 cells with siRNA against the β_1 integrin subunit (48 h) inhibited their subsequent attachment to HUVECs. *G*, flow cytometry analysis shows that siRNA against α_2 and α_3 integrin subunits reduced the expression of these integrins on MDA-MB-231 cells. *H*, adhesion of MDA-MB-231 cells to HUVECs was inhibited when MDA-MB-231 cells were treated with the indicated siRNA for 48 h. **, $p < 0.01$; ***, $p < 0.001$, *versus* control. Each experiment was independently performed 3–4 times. *Error bars*, S.E.

software (Olympus Soft Imaging Solutions, Golden, CO) with an Olympus BX61 motorized microscope (Olympus America, Center Valley, PA).

TEM Assay—A kit from Cell Biolabs, Inc. was used for TEM assays according to the manufacturer's instructions. MDA-MB-231 or MCF-7 cells (25×10^6 each) were resuspended in 1 ml of complete medium and incubated for 1 h at 37 °C in the presence of 50 μg/ml calcein-AM (Molecular Probes, Invitrogen). After the cells were labeled, they were resuspended at a concentration of 1×10^6 cells/ml in DMEM. MDA-MB-231 or MCF-7 cells (1.5×10^5 in 150 μl) were added to the upper compartment of transwell chambers with 6.5-mm diameter and 8-μm pores for 4 h. To remove non-migrating cells, the apical side of the filter was scraped gently with cotton wool and discarded; only cells that attached to the bottom side of the filter or migrating tumor cells were quantified with an Ultra384 plate reader (Tecan) by using 485- and 535-nm excitation and emission filters, respectively.

Statistics—Adhesion and transmigration data were analyzed by analysis of variance, and a two-sample Student *t* test was used to calculate statistical significance (Excel, Microsoft Corp., Houston, TX). All experiments were repeated at least three times. A probability (*P*) value of <0.05 was considered significant.

RESULTS

Attachment of Invasive Breast Cancer Cells (MDA-MB-231) to HUVECs Induces Tyr Phosphorylation of VE-cad, Dissociates β-Catenin from the VE-cad Complex, and Retracts Endothelial Cells—We recently showed that the interaction of monocytes with endothelial cells leads to Tyr phosphorylation of VE-cad and disruption of endothelial adherens junctions (14). To determine if the interaction of breast cancer cells with endothelial cells leads to similar effects on endothelial adherens junctions, invasive breast cancer cells (MDA-MB-231) were added to a monolayer of HUVECs. MDA-MB-231 cells are known as a highly aggressive estrogen receptor-negative breast cancer cell line. As indicated in Fig. 1*A*, VE-cad Tyr phosphorylation was significantly increased after the addition of MDA-MB-231 cells, and this was accompanied by an increase in the phosphorylation of Src and Pyk-2, two Tyr kinases that are involved in Tyr phosphorylation of VE-cad (14). The increase in VE-cad tyrosine phosphorylation induced by MDA-MB-231 cells also occurs after attachment of other invasive cancer cells (see below). siRNA against Src and Pyk2, which reduced basal levels of each respective protein almost 50% (data not shown), attenuated the Tyr phosphorylation of VE-cad induced by MDA-MB-231 cells (Fig. 1, *B* and *C*). As indicated by immunofluorescence staining of VE-cad (Fig. 1*D*), the attachment of MDA-MB-231 cells to a monolayer of HUVECs led to a dramatic retraction in endothelial cells, a process that may precede MDA-MB-231 endothelial transmigration. When HUVECs were pretreated with a Src inhibitor (4-amino-5-(4-chlorophenyl)-7-(*t*-butyl) pyrazolo[3,4-*d*]pyrimidine, PP2), the retraction of HUVECs was blocked (Fig. 1*D*), suggesting that Src activation contributes to MDA-MB-231-induced retraction of HUVECs. In addition, after the attachment of MDA-MB-231 cells to HUVECs, β-catenin was dissociated from VE-cad (Fig. 1*E*).

Adhesion of Breast Cancer Cells to HUVECs Depends on the Expression of β_1 Integrins on MDA-MB-231 Cells—Integrins regulate cell proliferation, migration, invasion, and survival, processes that are required in both tumorigenesis and metasta-

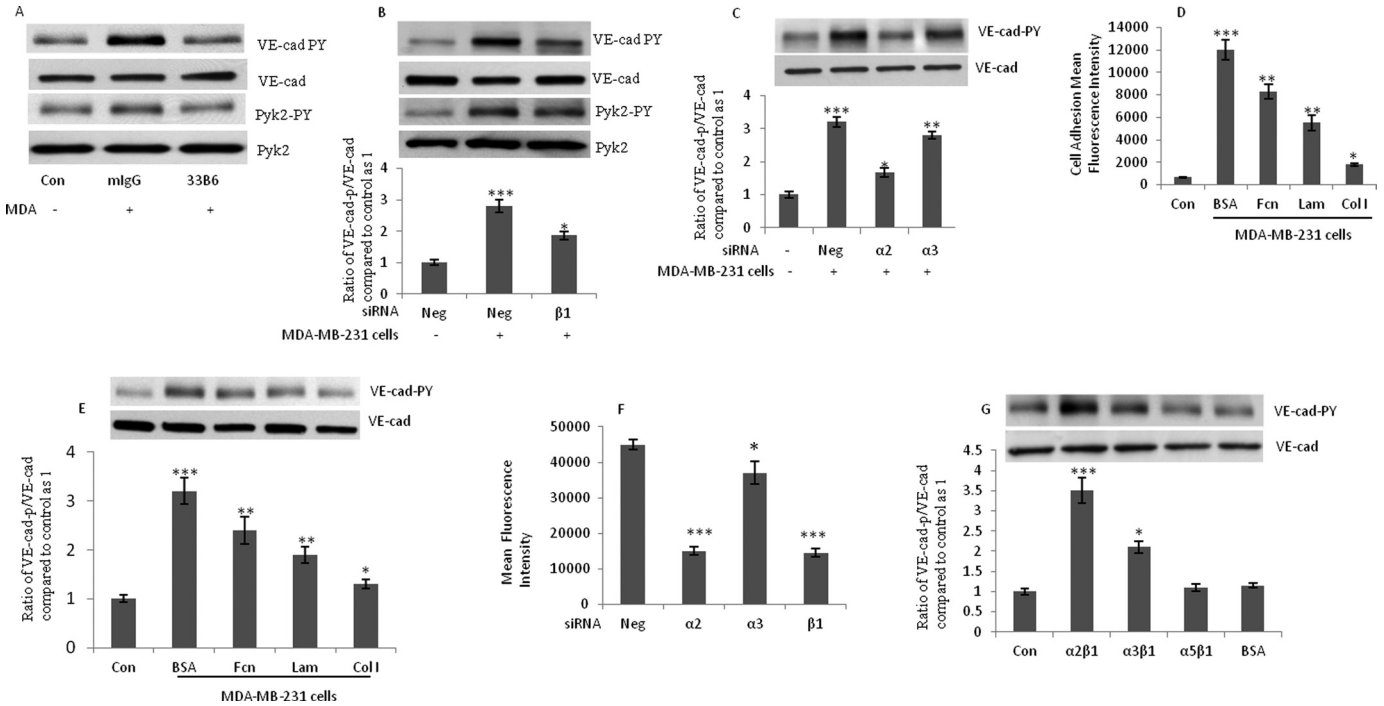

FIGURE 3. **Integrin $\alpha_2\beta_1$ on MDA-MB-231 cells mediates breast cancer cell-induced Tyr phosphorylation of VE-cad in HUVECs.** *A*, blocking antibody against β_1 integrin suppressed MDA-MB-231 cell-induced Tyr phosphorylation of VE-cad. MDA-MB-231 cells were treated with the β_1 integrin-blocking antibody (33B6; 1 μg/ml) for 1 h, washed, and added to HUVECs (3×10^6 MDA-MB-231 cells/1×10^6 HUVECs) for 5 min. *B* and *C*, integrin subunits α_2 and β_1 mediated breast cancer cell-induced Tyr phosphorylation of HUVECs. MDA-MB-231 cells were treated with siRNA against β_1 (*B*) or α_2 and α_3 (*C*) integrin subunits, and after 48 h, cells were added to HUVECs (3×10^6 MDA-MB-231 cells/1×10^6 HUVECs) for 5 min. *Neg*, scrambled siRNA control. *D*, adhesion of MDA-MB-231 cells to HUVECs was inhibited when MDA-MB-231 cells were treated with fibronectin, laminin, or collagen type I. MDA-MB-231 cells were incubated with 10 μM of fibronectin (*Fcn*), laminin (*Lam*), collagen type I (*Col I*), or bovine serum albumin (*BSA*) for 1 h; washed; and subjected to the adhesion assay. *E*, MDA-MB-231 cell-induced Tyr phosphorylation of VE-cad was attenuated by the pretreatment of MDA-MB-231 cells with collagen type I. MDA-MB-231 cells were treated with fibronectin, laminin, collagen type I, or BSA (10 μM each) and added to HUVECs (3×10^6 MDA-MB-231 cells/1×10^6 HUVECs) for 5 min. *F*, TEM of MDA-MB-231 cells was attenuated by siRNA against α_2 and β_1 integrin subunits. MDA-MB-231 cells were transfected with the indicated siRNA 48 h before their addition to HUVECs (10×10^5 cells/well). After 4 h, the migrating tumor cells were quantified with a plate reader by using 485- and 535-nm excitation and emission filters, respectively. Data are expressed as the mean ± S.D. (*error bars*) from triplicate experiments. *G*, recombinant human $\alpha_2\beta_1$ integrin induced Tyr phosphorylation of VE-cad. Recombinant human integrin $\alpha_2\beta_1$, $\alpha_3\beta_1$, or $\alpha_5\beta_1$ or BSA (5 μM each) were added to HUVECs for 5 min. *MDA*, MDA-MB-231 cells. *, $p < 0.05$; **, $p < 0.01$; ***, $p < 0.001$, *versus* control. Each experiment was independently performed 3–4 times.

sis of cancer cells. To determine which integrins mediate breast cancer cell-induced VE-cad Tyr phosphorylation, we examined integrin expression on MDA-MB-231 cells. As indicated in Fig. 2*A*, β_1 integrins were the most highly expressed integrins found on MDA-MB-231 cells. In addition, α_2 and α_3 integrin subunits were expressed at greater levels than the rest of the α integrin subunits examined. The expressions of α_5 and α_6 integrins were also significantly greater than the control IgG. The expression of α_4 integrin subunit was almost undetectable. The expression of $\alpha_v\beta_3$ integrins on MDA-MB-231 cells was very low. The expression of $\alpha_v\beta_3$ integrin on HUVECs was used as a positive control (Fig. 2*B*).

To determine whether β_1 integrins are critical for the adhesion of MDA-MB-231 cells to endothelial cells and for the induction of VE-cad Tyr phosphorylation in HUVECs, MDA-MB-231 cells were treated with a β_1 integrin-blocking antibody (mAb 33B6) or β_1 integrin-activating antibody (mAb TS2/16). The results of substrate attachment assays showed that the pretreatment of MDA-MB-231 cells with β_1 integrin-blocking (33B6) antibody or β_1 integrin-activating (TS2/16) antibody inhibited or enhanced, respectively, the attachment of these cells to laminin, fibronectin, and collagen type I (Fig. 2*C*). The attachment of MDA-MB-231 cells to HUVECs was inhibited or enhanced when MDA-MB-231 cells were treated with the β_1 integrin-blocking (33B6) antibody or β_1 integrin-activating (TS2/16) antibody, respectively (Fig. 2*D*). To verify the data obtained with the function-blocking mAb 33B6, we examined the effects of knocking down the β_1 integrin subunit in MDA-MB-231 cells with siRNA. The knockdown of the β_1 integrin subunit was confirmed by flow cytometry (Fig. 2*E*). The adhesion of MDA-MB-231 cells to HUVECs was reduced by β_1 siRNA (Fig. 2*F*), suggesting that β_1 integrins play a critical role in the attachment of MDA-MB-231 cells to HUVECs. To determine which α subunit was involved in the attachment of MDA-MB-231 cells to HUVECs, we examined the effects of knocking down α_2 and α_3 integrin subunits in MDA-MB-231 cells. By using flow cytometry, we confirmed the siRNA-mediated reduction in expression of α_2 and α_3 integrin subunits (Fig. 2*G*). The inhibition of α_2 subunit did not show any effect on expression of α_3 subunit and vice versa (data not shown). As shown in Fig. 2*H*, α_2 and α_3 siRNAs inhibited the adhesion of MDA-MB-231 cells to HUVECs (Fig. 2*H*). The inhibition was more pronounced for α_2 siRNA.

MDA-MB-231 Cell-induced Tyr Phosphorylation of VE-cad in HUVECs Is Mediated by β_1 and α_2 Integrins—Previous studies have shown that the interaction of integrins $\alpha_4\beta_1$ and

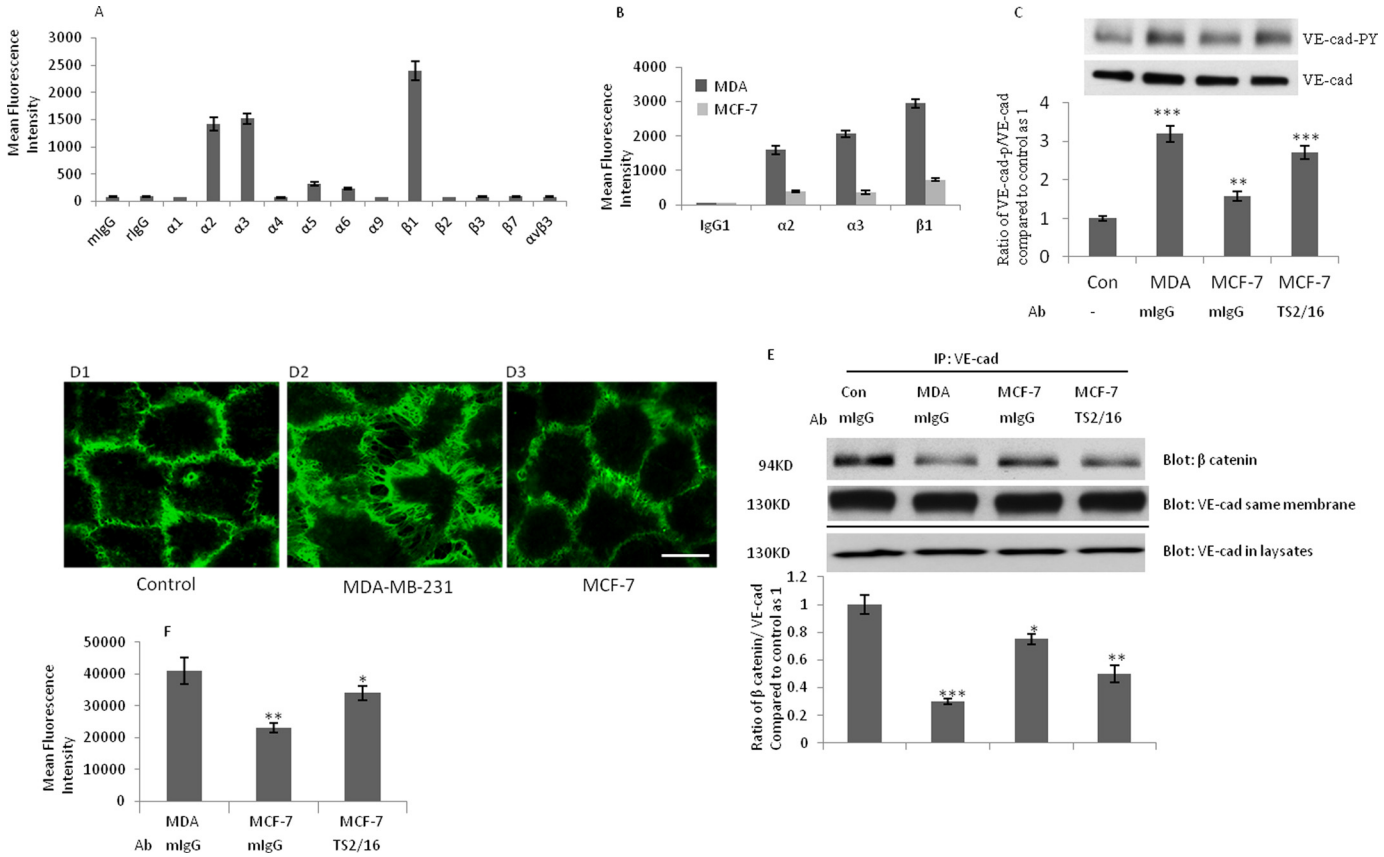

FIGURE 4. **Noninvasive breast cancer cells (MCF-7) induce VE-cad Tyr phosphorylation to a lesser degree than invasive breast cancer cells (MDA-MB-231).** *A*, flow cytometry analysis shows the integrin expression profile of MCF-7 cells. *mIgG*, mouse IgG; *rIgG*, rat IgG. *B*, expression of β_1, α_2, and α_3 integrin subunits was lower in MCF-7 cells than in MDA-MB-231 cells. *C*, VE-cad Tyr phosphorylation induced by MCF-7 cells was less than that induced by MDA-MB-231 cells. MCF-7 or MDA-MB-231 cells (3×10^6 cancer cells/1×10^6 HUVECs) were added to HUVECs for 5 min. MCF-7 cells were treated with β_1 integrin-activating antibody (TS2/16; 1 μg/ml) for 1 h, washed, and added to HUVECs. *D*, induction of endothelial retraction by MCF-7 cells is much lower than that by MDA-MB-231 cells. MDA-MB-231 and MCF-7 cells were trypsinized, washed, and added to HUVECs for 10 min. Cells were fixed with 4% paraformaldehyde and stained with primary rabbit polyclonal antibody against VE-cad and secondary FITC-conjugated goat anti-rabbit IgG antibody (*green*). *D1*, control HUVECs without the addition of MDA-MB-231 cells. *D2*, retraction of HUVECs 10 min after the addition of MDA-MB-231 cells (3×10^6 MDA-MB-231 cells/1×10^6 HUVECs). *D3*, the addition of MCF-7 cells to HUVECS for 10 min (3×10^6 MCF-7 cells/1×10^6 HUVECs). *Bar*, 10 μm. *E*, the dissociation of β-catenin from VE-cad induced by MCF-7 cells was less than that induced by MDA-MB-231 cells. MCF-7 or MDA-MB-231 cells (3×10^6 cancer cells/1×10^6 HUVECs) were added to HUVECs for 5 min, and HUVECs were used for immunoprecipitation assays. *F*, fewer MCF-7 cells than MDA-MB-231 cells crossed endothelial cells in the transwell chamber assay. MCF-7 cells were treated with β_1 integrin-activating antibody (TS2/16; 1 μg/ml) or mIgG (1 μg/ml) for 1 h, washed, and used for the TEM assay. *MDA*, MDA-MB-231 cells. *, $p < 0.05$; **, $p < 0.01$; ***, $p < 0.001$, *versus* control. Each experiment was independently performed 3–4 times. *Error bars*, S.E.

$\alpha_{L/M}\beta_2$ with VCAM-1 and ICAM-1 adhesion molecules leads to monocyte-induced Tyr phosphorylation of VE-cad (14, 16). By using blocking antibody and siRNA, we sought to determine which integrin(s) mediate MDA-MB-231 cell-induced Tyr phosphorylation of VE-cad in HUVECs. The treatment of MDA-MB-231 cells with blocking antibody against β_1 integrin suppressed MDA-MB-231 cell-induced Tyr phosphorylation of VE-cad and Pyk2 (Fig. 3*A*). The treatment of MDA-MB-231 cells with siRNA against β_1 and α_2 integrin subunits attenuated Tyr phosphorylation of VE-cad in HUVECs (Fig. 3, *B* and *C*). Tyr phosphorylation of VE-cad was slightly but significantly reduced by siRNA against α_3 integrin subunit. The siRNA-mediated knockdown of α_4, α_5, α_6, β_2, and $\alpha_v\beta_3$ integrin subunits failed to attenuate breast cancer cell-induced Tyr phosphorylation of VE-cad (data not shown). To determine which ligand(s) mediates MDA-MB-231-induced Tyr phosphorylation of HUVECs, we pretreated MDA-MB-231 cells with soluble laminin, fibronectin, or collagen type I before adding the cells to a monolayer of HUVECs. As shown in Fig. 3*D*, the adhesion of MDA-MB-231 cells to HUVECs was partially inhibited by the pretreatment of MDA-MB-231 cells with laminin/fibronectin and profoundly inhibited by collagen type I. VE-cad Tyr phosphorylation in HUVECs was primarily attenuated by collagen type I and weakly attenuated by laminin and fibronectin (Fig. 3*E*). TEM of MDA-MB-231 cells was also inhibited by the siRNA-mediated knockdown of α_2 and β_1 integrin subunits (Fig. 3*F*). Integrin $\alpha_2\beta_1$-mediated adhesion of MDA-MB-231 cells to HUVECs could induce VE-cad Tyr phosphorylation. To determine whether $\alpha_2\beta_1$ integrin alone is sufficient to induce this, we treated HUVECs with recombinant soluble integrins ($\alpha_2\beta_1$, $\alpha_3\beta_1$, and $\alpha_5\beta_1$) and examined tyrosine phosphorylation of VE-cad. As shown in Fig. 3*G*, recombinant human $\alpha_2\beta_1$ and to a lesser degree $\alpha_3\beta_1$ integrins induced Tyr phosphorylation of VE-cad in HUVECs, whereas recombinant human $\alpha_5\beta_1$ or BSA did not. These results suggest that binding of $\alpha_2\beta_1$ and $\alpha_3\beta_1$ integrins to HUVECs is sufficient to induce Tyr phosphorylation of HUVECs and that MDA-MB-231 cell-induced Tyr phosphorylation of VE-cad is primarily mediated by the integrin $\alpha_2\beta_1$.

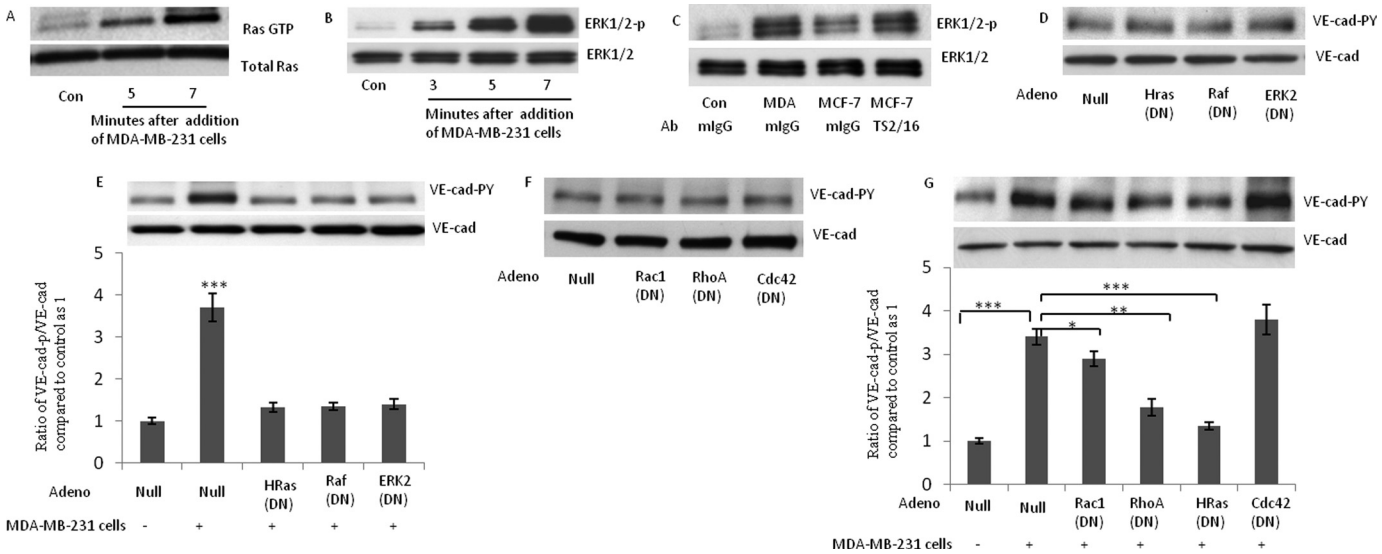

FIGURE 5. **Breast cancer cell-induced Tyr phosphorylation of VE-cad is mediated by activation of the H-Ras/Raf/MEK/ERK signaling cascade.** *A*, attachment of MDA-MB-231 cells to HUVECs activated Ras. A pull-down assay was used to assess the binding of GTP to Ras. *B*, MDA-MB-231 cells induced phosphorylation of ERK in HUVECs. MDA-MB-231 cells (3×10^6 MDA-MB-231 cells/1×10^6 HUVECs) were added to HUVECs for the indicated times. *C*, MCF-7 cells induce endothelial cell ERK phosphorylation to a lower degree than MDA-MB-231 cells. MCF-7 cells and MDA-MB-231 cells (3×10^6 tumor cells/1×10^6 HUVECs) were added to HUVECs for 5 min. In the indicated sample, MCF-7 cells were treated with β_1 integrin-activating antibody (TS2/16; 1 μg/ml) for 1 h, washed, and then added to HUVECs. *D*, dominant negative forms of H-Ras, Raf-1, and ERK2 did not show any effect on the basal levels of VE-cad Tyr phosphorylation in HUVECs. HUVECs were transduced with the indicated adenovirus and were collected after 48 h. *E*, MDA-MB-231 cell-induced Tyr phosphorylation of VE-cad was attenuated when H-Ras, Raf-1, or ERK2 was inhibited. HUVECs were transduced with the indicated adenovirus, and after 48 h, MDA-MB-231 cells (3×10^6 MDA-MB-231 cells/1×10^6 HUVECs) were added to HUVECs for 5 min. *F*, inhibition of RhoA, Rac-1, and CDC42 with their respective dominant negative forms did not attenuate the basal level of Tyr phosphorylation of VE-cad. HUVECs were transduced with the indicated adenovirus, and after 48 h, MDA-MB-231 cells (3×10^6 MDA-MB-231 cells/1×10^6 HUVECs) were added to HUVECs for 5 min. *G*, inhibition of RhoA attenuates MDA-MB-231 cell-induced Tyr phosphorylation of VE-cad. HUVECs were transduced with the indicated adenovirus, and after 48 h, MDA-MB-231 cells (3×10^6 MDA-MB-231 cells/1×10^6 HUVECs) were added to HUVECs for 5 min. *MDA*, MDA-MB-231 cells. *, $p < 0.05$; **, $p < 0.01$; ***, $p < 0.001$, *versus* control. Each experiment was independently performed 3–4 times. *Error bars*, S.E.

Weakly Invasive Breast Cancer Cells (MCF-7) Induce VE-cad Tyr Phosphorylation to a Lesser Degree than Highly Invasive Breast Cancer Cells (MDA-MB-231)—To determine whether the invasiveness of breast cancer cells affects the induction of VE-cad Tyr phosphorylation in HUVECs, we compared the effects of highly invasive MDA-MB-231 cells with those of weakly invasive MCF-7 cells. In MCF-7 cells, integrin subunits, including β_1, α_2, and α_3, were expressed 3–4-fold less than in MDA-MB-231 cells (Fig. 4, *A* and *B*). In addition, MCF-7 cells induced less VE-cad Tyr phosphorylation in HUVECs than did MDA-MB-231 cells (Fig. 4*C*). However, VE-cad Tyr phosphorylation was increased by the treatment of MCF-7 cells with β_1 integrin-activating antibody (TS2/16) (Fig. 4*C*). In addition, interaction of MCF-7 with HUVECs did not induce endothelial retraction to the extent that MDA-MB-231 cells did (Fig. 4*D*). MCF-7 cells also induced less dissociation of β-catenin from the VE-cad complex than did MDA-MB-231 cells (Fig. 4*E*). The low potency of MCF-7 in induction of VE-cad Tyr phosphorylation correlated with the TEM of MCF-7 cells, which was less than that of MDA-MB-231 cells (Fig. 4*F*). As shown in Fig. 4*F*, the TEM of MCF-7 cells increased after treatment with β_1 integrin-activating antibody (TS2/16).

MDA-MB-231 Cell-induced Tyr Phosphorylation of VE-cad Is Mediated by Activation of the H-Ras/Raf/MEK/ERK Signaling Cascade—We recently demonstrated that monocyte-induced Tyr phosphorylation of VE-cad is mediated by the H-Ras/Raf/MEK/ERK signaling cascade and requires MLC phosphorylation within HUVECs (14). In addition, we showed that the activation of H-Ras by using a constitutively active form of H-Ras or induction of the phosphorylation of MLC by inhibiting MLC phosphatase leads to Tyr phosphorylation of VE-cad and retraction of endothelial cells and enhances the TEM of monocytes (14). Here, we examined whether the H-Ras/Raf/MEK/ERK signaling cascade governs MDA-MB-231 cell-induced Tyr phosphorylation of VE-cad. Using a pull-down assay, we showed that the attachment of MDA-MB-231 cells to HUVECs increased the GTP-bound form of Ras (Fig. 5*A*) and ERK phosphorylation (Fig. 5*B*). In addition, MCF-7 cells induced less ERK phosphorylation in HUVECs than did MDA-MB-231 cells (Fig. 5*C*), which was reversed by the treatment of MCF-7 cells with β_1 integrin-activating antibody (TS2/16) (Fig. 5*C*). To determine whether activation of the H-Ras/Raf/MEK/ERK signaling cascade is required for MDA-MB-231 cell-induced Tyr phosphorylation of VE-cad, H-Ras, Raf-1, and ERK-2 were each inhibited by recombinant DN adenovirus. The inhibitory activity of each DN form of H-Ras, Raf-1, and ERK-2 was confirmed by the attenuation of IL-1-induced ERK phosphorylation in the presence of each recombinant adenovirus (data not shown). The DN forms of H-Ras, Raf-1, and ERK did not have a significant effect on the basal level of VE-cad Tyr phosphorylation in HUVECs (Fig. 5*D*). As shown in Fig. 5*E*, Tyr phosphorylation of VE-cad induced by MDA-MB-231 cells was almost completely blocked in HUVECs expressing DN H-Ras, Raf-1, or ERK-2. We recently revealed that H-Ras-induced VE-cad Tyr phosphorylation partially depends on RhoA (17). It has been demonstrated that constitutively active forms of Rac and RhoA synergize with the constitutively active form of Raf to activate ERK2, and a dominant negative mutant of Rac or RhoA

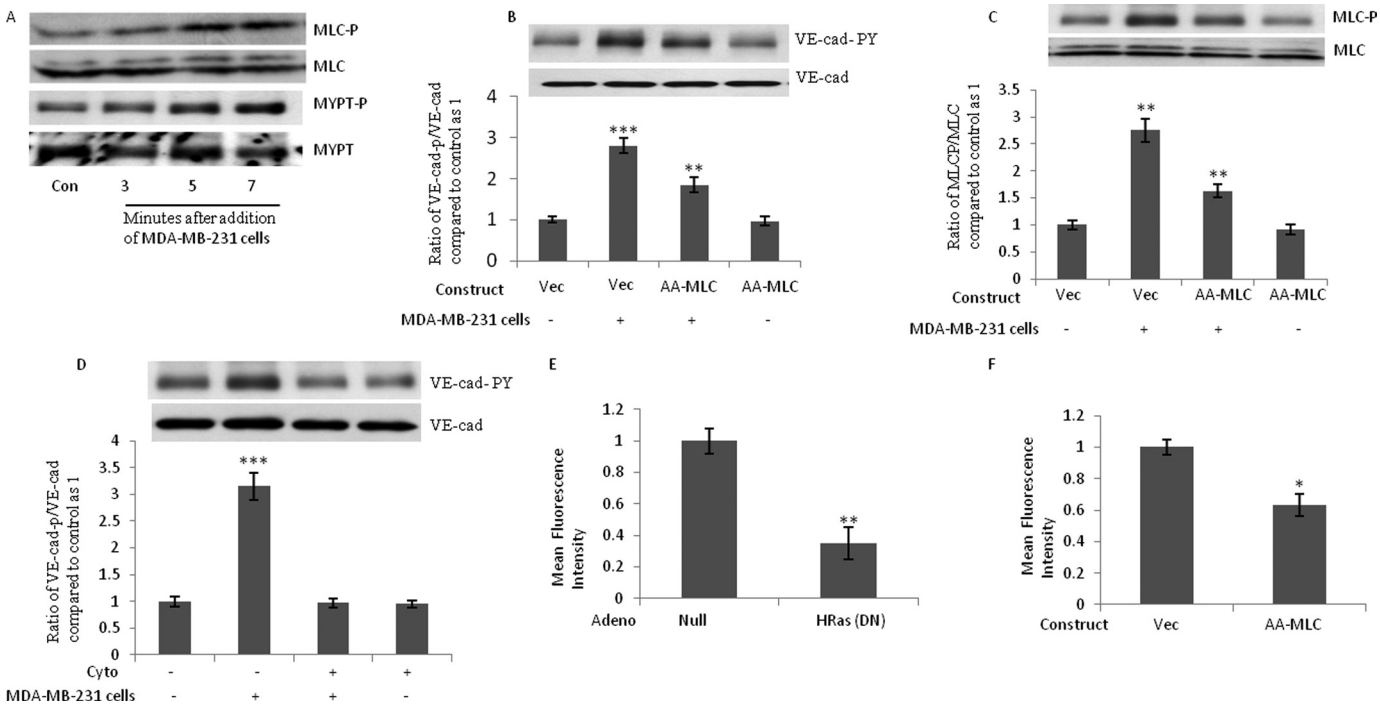

FIGURE 6. **Phosphorylation of MLC is required for breast cancer cell-induced Tyr phosphorylation of VE-cad.** *A*, phosphorylation of MLC and MLC phosphatase (*MYPT*) after the attachment of MDA-MB-231 cells. MDA-MB-231 cells (3×10^6 MDA-MB-231 cells/1×10^6 HUVECs) were added to HUVECs for the indicated times. *B* and *C*, MDA-MB-231 cell-induced VE-cad Tyr phosphorylation and MLC phosphorylation were attenuated when A-A-MLC was overexpressed in HUVECs. HUVECs were transfected by the indicated constructs. After 48 h, MDA-MB-231 cells (3×10^6 MDA-MB-231 cells/1×10^6 HUVECs) were added to HUVECs for 5 min. *D*, MDA-MB-231 cell-induced Tyr phosphorylation of VE-cad was suppressed when HUVECs were treated with cytochalasin D. HUVECs were treated with 1 μM cytochalasin D for 2 h, and MDA-MB-231 cells (3×10^6 MDA-MB-231 cells/1×10^6 HUVECs) were added to HUVECs for 5 min. *E* and *F*, TEM of MDA-MB-231 cells was inhibited when H-Ras activity or MLC phosphorylation was inhibited. HUVECs were transduced by the indicated adenovirus or were transfected by the indicated constructs. After 48 h, cells were used to analyze the TEM of MDA-MB-231 cells. *, $p < 0.05$; **, $p < 0.01$; ***, $p < 0.001$, *versus* control. Each experiment was independently performed 3–4 times. *Error bars*, S.E.

can attenuate Raf activation by Ras (18–20). To determine the role of Rho family GTPases in MDA-MB-231 cell-induced VE-cad Tyr phosphorylation, recombinant DN forms of RhoA, Rac1, and Cdc42 were used. Pull-down assays confirmed the inhibitory effects of DN-RhoA, DN-Rac1, and DN-Cdc42 recombinants (data not shown). Overexpression of DN-RhoA, DN-RAC1, and DN-Cdc42 did not alter the basal level of VE-cad Tyr phosphorylation in HUVECs (Fig. 6*F*). Inhibition of RhoA by the DN form attenuated MDA-MB-231 cell-induced Tyr phosphorylation of VE-cad (Fig. 5*F*). In contrast to the inhibition of Cdc42, which did not attenuate Tyr phosphorylation of VE-cad, inhibition of Rac1 slightly but significantly attenuated Tyr phosphorylation of VE-cad (Fig. 5*F*).

Phosphorylation of MLC Is Required for MDA-MB-231 Cell-induced Tyr Phosphorylation of VE-cad—Disruption of endothelial barrier function by proinflammatory agents is associated with alteration in endothelial cytoskeleton and phosphorylation of MLC (21). Our group recently delineated that MLC phosphorylation is adequate to induce Tyr phosphorylation of VE-cad (14). We previously demonstrated that inhibition of MLC phosphorylation attenuates VE-cad tyrosine phosphorylation induced by the constitutively active form of H-Ras (17). Therefore, the role of MLC phosphorylation and actin polymerization in MDA-MB-231 cell-induced Tyr phosphorylation was studied. After the attachment of MDA-MB-231 cells to HUVECs, MLC phosphorylation in the endothelial cells was induced. This was accompanied by the inhibition/phosphorylation of MYPT (the regulatory subunit of MLC phosphatase; Fig. 6*A*). To determine whether MLC phosphorylation is critical for the Tyr phosphorylation of VE-cad induced by MDA-MB-231 cells, we used a dominant negative mutant of MLC (A-A-MLC) that cannot be phosphorylated (14). The transfection rate for the pcDNA3.1/CT-GFP constructs was 40% (data not shown). Consistent with a previous report (14), the overexpression of A-A-MLC in HUVECs did not alter basal levels of MLC phosphorylation (Fig. 6*C*). However, MLC phosphorylation and VE-cad Tyr phosphorylation induced by MDA-MB-231 cells were attenuated when A-A-MLC was overexpressed in HUVECs (Fig. 6, *B* and *C*).

Alterations in actin-cytoskeleton structures and dynamics affect TEM of leukocytes (22). We previously showed that MLC phosphorylation leads to the polymerization of G actin and the formation of F actin (23). To determine whether the polymerization of actin plays a role in the Tyr phosphorylation of VE-cad induced by MDA-MB-231 cells, we treated HUVECs with cytochalasin D, an inhibitor of actin polymerization. Tyr phosphorylation of VE-cad induced by MDA-MB-231 cells was suppressed when HUVECs were treated with cytochalasin D (Fig. 6*D*). We also examined the effects of dominant negative H-Ras and the inhibition of MLC phosphorylation by A-A-MLC on the TEM of MDA-MB-231 cells. As shown in Fig. 6, *E* and *F*, the TEM of MDA-MB-231 cells were inhibited by dominant negative H-Ras and by the transfection of HUVECs with A-A-MLC. These experiments indicate the critical role of H-Ras activation

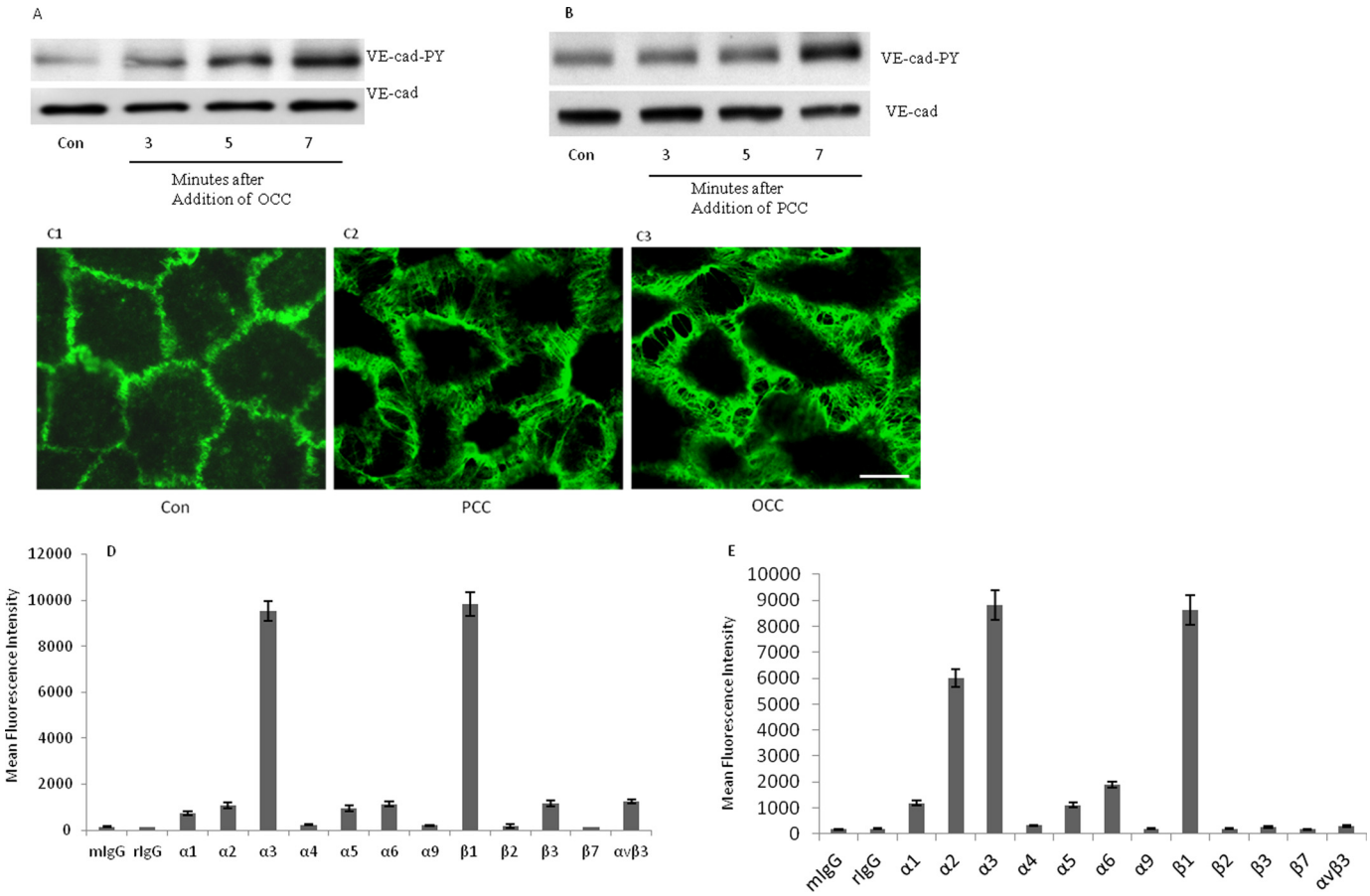

FIGURE 7. **Attachment of invasive ovarian and prostatic cancer cells to HUVECs induces Tyr phosphorylation of VE-cad.** *A* and *B*, attachment of ovarian (SKOV3; ovarian cancer cells (*OCC*)) and prostatic (PC-3; prostatic cancer cells (*PCC*)) cancer cells to HUVECs induced Tyr phosphorylation of VE-cad. SKOV3 and PC-3 cells (3×10^6 cancer cells/1×10^6 HUVECs) were added to HUVECs for the indicated times. *C*, endothelial cells were retracted after attachment of PC-3 and SKOV3 cells. PC-3 (*C2*) and SKOV3 (*C3*) cells were added to HUVECs (3×10^6 cancer cells/1×10^6 HUVECs), and after 10 min, HUVECs were fixed and used for immunofluorescence staining. *Bar*, 10 μm. *D* and *E*, flow cytometry analysis showing integrin expression profiles for SKOV3 and PC-3 cells. Each experiment was independently performed 3–4 times. *Error bars*, S.E.

and MLC phosphorylation in HUVECs for TEM of MDA-MB-231 cells. Our results suggest that MDA-MB-231 cell-induced VE-cad Tyr phosphorylation in HUVECs resembles VE-cad Tyr phosphorylation induced by monocytes and is mediated by H-Ras activation and MLC phosphorylation.

Attachment of Invasive Ovarian and Prostatic Cancer Cells to HUVECs Induces Tyr Phosphorylation of VE-cad—To determine whether the disruption of endothelial adherens junctions occurs after the attachment of other invasive cancer cells, we studied ovarian (SKOV3) and prostatic (PC-3) invasive cancer cells. As shown in Fig. 7, *A* and *B*, the addition of both SKOV3 and PC-3 and cells to HUVECs increased Tyr phosphorylation of VE-cad. In addition, endothelial cells retracted after the attachment of PC-3 and SKOV3 cells to HUVECs (Fig. 7*C*). Integrin expression profiles for SKOV3 and PC-3 cells were similar to those for MDA-MB-231 cells, with a higher expression of β_1, α_2, and α_3 integrin subunits (Fig. 7, *D* and *E*). However, the relative expression of α_2 integrin subunit by SKOV3 cells was not as high as the other studied cancer cell lines. In addition, in contrast to PC-3 and MDA-MB-231 cells, SKOV3 cells expressed integrin $\alpha_v\beta_3$ to a higher extent (Fig. 7*D*). When SKOV3 and PC-3 and cells were pretreated with β_1 blocking antibody, their induction of Tyr phosphorylation of VE-cad in HUVECs were suppressed (Fig. 8, *A* and *B*). Flow cytometry analysis indicated that siRNA against β_1 integrin subunit reduced the expression of this integrin almost 40–50% in both PC-3 and SKOV3 cells (data not shown). The siRNA-mediated knockdown of β_1 in SKOV3 and PC-3 cells attenuated the SKOV3 and PC-3 cell-induced Tyr phosphorylation of VE-cad in HUVECs (Fig. 8, *C* and *D*). Furthermore, dominant negative H-Ras, Raf1, and ERK2 attenuated SKOV3 and PC-3 cell-induced Tyr phosphorylation of VE-cad (Fig. 8, *E* and *F*).

DISCUSSION

In this study, we have shown that the attachment of invasive breast cancer cells to endothelial cells leads to VE-cad Tyr phosphorylation and dissociation of β-catenin from the VE-cad complex. The induction of VE-cad Tyr phosphorylation by MDA-MB-231 cells is mainly triggered by $\alpha_2\beta_1$ integrin, is mediated by the H-Ras/Raf/MEK/ERK signaling cascade, and depends on MLC phosphorylation. Furthermore, the attachment of invasive ovarian and prostatic cancer cells to HUVECs similarly altered endothelial signal transduction. Our results provide evidence that invasive breast cancer cells (MDA-MB-231 cells) are involved in intraendothelial signaling that promotes the TEM of cancer cells. Our study suggests that leuko-

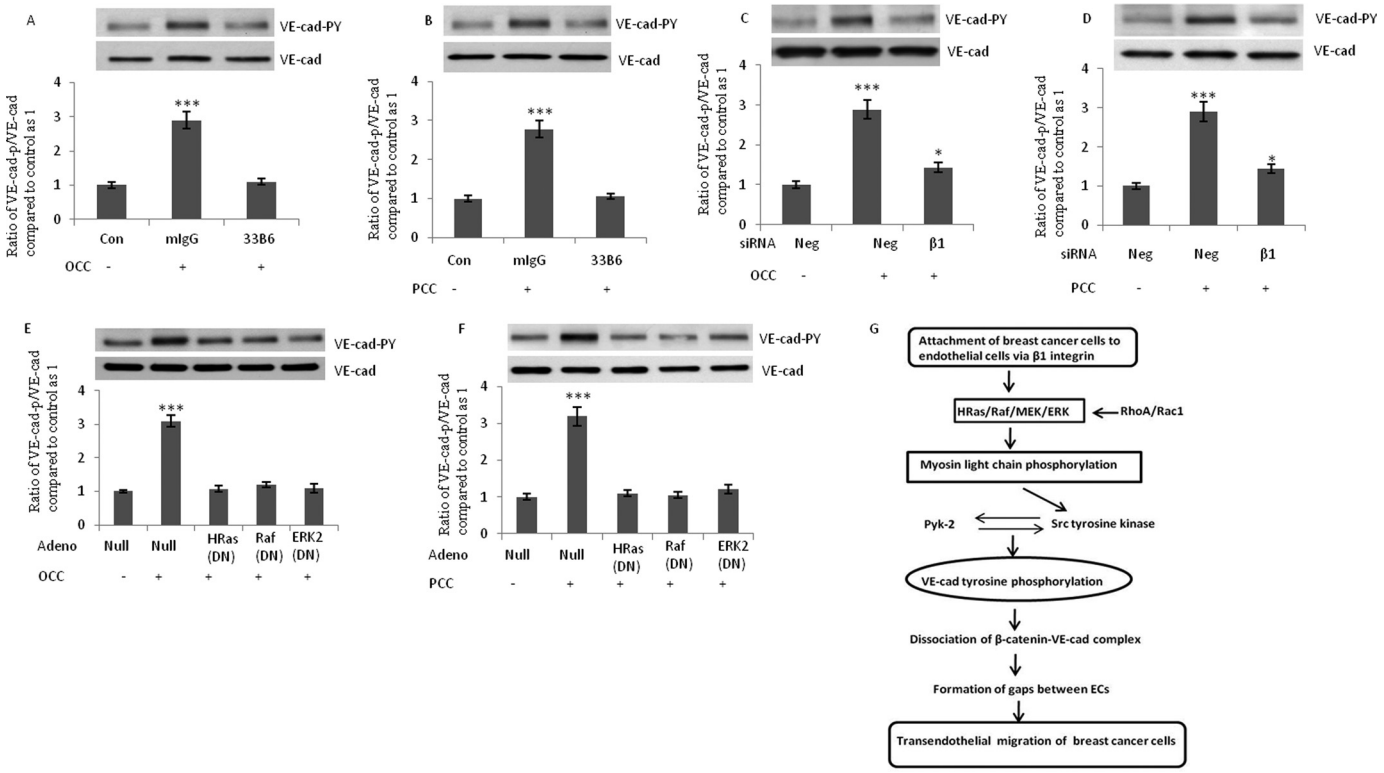

FIGURE 8. **Induction of endothelial cells VE-cad Tyr phosphorylation by ovarian and prostatic cancer cells is mediated by β_1 integrin and requires H-Ras.** *A* and *B*, blocking antibody against β_1 integrin suppressed SKOV3 and PC-3 cell-induced Tyr phosphorylation of VE-cad. SKOV3 and PC-3 cells were treated with the β_1 integrin-blocking antibody (33B6; 1 μg/ml) for 1 h, washed, and added to HUVECs (3×10^6 tumor cells/1×10^6 HUVECs) for 5 min. *C* and *D*, knockdown of β_1 integrin subunit attenuated SKOV3 and PC-3 cell-induced Tyr phosphorylation of VE-cad. SKOV3 (ovarian cancer cells; *OCC*) and PC-3 (prostatic cancer cells; *PCC*) cells were transfected with the indicated siRNA. After 48 h, cells were added to HUVECs (3×10^6 cancer cells/1×10^6 HUVECs) for 5 min. *Neg*, scrambled siRNA control. *E* and *F*, dominant negative form of H-Ras, Raf, and ERK2 attenuated SKOV3 and PC-3 cell-induced VE-cad Tyr phosphorylation in HUVECs. HUVECs were transduced with the indicated adenovirus and were collected after 48 h. SKOV3 and PC-3 cells (3×10^6 cancer cells/1×10^6 HUVECs) were added to HUVECs for 5 min. *G*, a hypothetical model for the alterations in signal transduction of HUVECs after attachment of breast cancer cells. Attachment of invasive breast cancer cells to endothelial cells via α_1 integrin initiates the signal transduction that leads to tyrosine phosphorylation of VE-cad. This disrupts the integrity of endothelial adherens junction and facilitates transendothelial migration of breast cancer cells. *, $p < 0.05$; **, $p < 0.01$; ***, $p < 0.001$, *versus* control. Each experiment was independently performed 3–4 times. *Error bars*, S.E.

cytes and invasive breast cancer cells (MDA-MB-231 cells) similarly induce alterations in endothelial cells that facilitate invasive cell diapedesis.

The role of $\alpha_2\beta_1$ integrin in the metastasis of cancer cells is not clear. Ramirez *et al.* (24) showed in a mouse model of breast cancer that $\alpha_2\beta_1$ integrin suppressed metastasis. In contrast, other studies have suggested that $\alpha_2\beta_1$ integrin may enhance metastasis to different organs (25–28). Wu *et al.* (29) reported that the knockdown of RhoA in MDA-MB-231 cells increased the invasive and proliferative properties of cells more than the knockdown of RhoC. Furthermore, the knockdown of RhoC in MDA-MB-231 cells resulted in low surface expression of α_2 and β_1 integrin subunits and prevented the cells from adhering to collagen type I, providing an explanation for their reduced motility and invasiveness. Indeed, other groups have shown that in prostate cancer, elevated levels of RhoC enhance collagen I-$\alpha_2\beta_1$ signaling and promote tumor metastasis to the bone matrix, which contains abundant levels of collagen type I (30, 31). In addition, the attachment of MDA-MB-231 cells to cortical bone disks was blocked by as much as 75% when cells were pretreated with monoclonal antibodies to α_2 and β_1 subunits of the integrin family (32).

We observed that the expression of β_1, α_2, and α_3 integrin subunits was higher in MDA-MB-231 cells than in MCF-7 cells (Fig. 4*B*). In support of our findings, a previous study showed that MDA-MB-231 cells expressed higher levels of $\alpha_2\beta_1$ than MCF-7 breast cancer cells (33). The critical role of VE-cad in the metastasis of cancer cells has been demonstrated. Disruption of the endothelial barrier directly with anti-VE-cad antibody amplified the metastasis of tumor cells in mice (5). In addition, Tyr phosphorylation of VE-cad by VEGF significantly increased the penetration of highly metastatic MDA-MB-231 breast cancer cells across the microvascular endothelial cell monolayer in human brain tissue (34). Furthermore, Weis *et al.* (5) proposed a model in which metastatic tumor cells release high levels of VEGF, which deregulate endothelial cell-cell junctional complexes and facilitate their extravasation. Our results support a model in which, in addition to the release of VEGF by cancer cells, the attachment of tumor cells to endothelial cells contributes to the disruption of endothelial adherens junctions and accelerates tumor cell TEM (Fig. 8*H*).

We have previously shown that the activation of Ras/ERK leads to MLC phosphorylation and that MLC phosphorylation leads to VE-cad Tyr phosphorylation (14). Our findings in the present study further indicate that inhibiting MLC phosphorylation and blocking G actin polymerization inhibits VE-cad Tyr phosphorylation and the TEM of MDA-MB-231 cells. In line with these findings, blocking endothelial MLC phosphorylation

has been shown to reduce the invasion of breast cancer cells (35). How phosphorylation of MLC leads to VE-cad Tyr phosphorylation needs further investigation. Actomyosin contraction could trigger not only mechanical and cytoskeletal changes in endothelial cells but could also lead to the redistribution of kinases and phosphatases within the cells. This mechanism might participate in the phosphorylation of VE-cad and associated proteins in response to tumor cell adhesion to endothelial cells. We demonstrated that attachment of monocytes to endothelial cells or overexpression of CA-H-Ras in endothelial cells recruits Src to the VE-cad complex (14, 17). Furthermore, the earlier findings demonstrated that actin polymerization, Rho A activity, and activity of myosin are required for recruitment and accumulation of junctional complex components (36, 37).

Our study suggests that MDA-MB-231 cell-induced VE-cad Tyr phosphorylation is primarily mediated by the interaction of $\alpha_2\beta_1$ integrin on invasive cancer cells and a counterligand on endothelial cells. Breast cancer cells may attach to subendothelium extracellular matrix. Several studies, both *in vitro* and *in vivo*, have shown that endothelial cells retract before tumor cell extravasation. Nicolson (38) reported that melanoma cells induce endothelial cell retraction, creating a portal of transmigration. Such endothelial cell retraction has also been described in pancreatic (39), lung (40), and breast (41) cancer cells. After tumor cell attachment, endothelial cell retraction is initiated, and tumor cells spread on the exposed subendothelial matrix. Future investigation that addresses whether the retraction of endothelial cells precedes breast cancer cell-induced VE-cad Tyr phosphorylation (or vice versa) will be very informative. It is also possible that tumor cells attach to the components of the extracellular matrix that are attached to the surface of endothelial cells. Scanning electron microscopic analysis demonstrated that prostate cancer cells adhered directly to the endothelial cells and not to the underlying substrata (41). In addition, the presence of extracellular matrix components on the surface of endothelial cells has been reported (42). Our data indicating that recombinant human $\alpha_2\beta_1$ or $\alpha_3\beta_1$ integrins are sufficient to reproduce MDA-MB-231 cell-induced Tyr phosphorylation of VE-cad support the concept that integrin interactions with yet undefined ligand on endothelial cells or on matrix that can be presented on the surface of endothelial cells directly cause endothelial cell retraction.

Our results showed that β_1 integrin triggered ovarian and prostatic cancer cell-induced VE-cad Tyr phosphorylation. This suggests the common alterations in endothelial signal transduction after attachment of breast, ovarian and prostatic invasive cancer cells. However, more specific studies are needed to investigate the molecular mechanisms that regulate the effects of ovarian and prostatic cancer cell attachment on endothelial cell signal transduction.

In conclusion, we have shown that the attachment of MDA-MB-231 cells to endothelial cells led to significant biochemical alterations in endothelial cells that facilitate the TEM of invasive breast cancer cells. Furthermore, we have shown that after the attachment of MDA-MB-231 cells, activation of the H-Ras/Raf/ERK signaling cascade and phosphorylation of MLC were required for integrin $\alpha_2\beta_1$-mediated disruption of endothelial adherens junctions. This study provides new insight into how the endothelial signaling cascade might be modulated by invading breast cancer cells and highlights the importance of examining the process of tumor invasion from the important yet underexplored perspective of the underlying endothelium.

Acknowledgments—We thank Dr. Andreas Kapus (University of Toronto) for generously providing the A-A-MLC construct, Dr. Bradley McIntyre (University of Texas MD Anderson Cancer Center, Houston, TX) for generously providing β_1 integrin-blocking mAb (33B6), and Nicole Stancel, Ph.D., ELS (Texas Heart Institute at St. Luke's Episcopal Hospital, Houston, TX) for editorial assistance.

REFERENCES

1. Akiyama, S. K., Olden, K., and Yamada, K. M. (1995) Fibronectin and integrins in invasion and metastasis. *Cancer Metastasis Rev.* **14,** 173–189
2. Nicolson, G. L. (1988) Organ specificity of tumor metastasis. Role of preferential adhesion, invasion, and growth of malignant cells at specific secondary sites. *Cancer Metastasis Rev.* **7,** 143–188
3. Alcaide, P., Newton, G., Auerbach, S., Sehrawat, S., Mayadas, T. N., Golan, D. E., Yacono, P., Vincent, P., Kowalczyk, A., and Luscinskas, F. W. (2008) p120-catenin regulates leukocyte transmigration through an effect on VE-cadherin phosphorylation. *Blood* **112,** 2770–2779
4. Potter, M. D., Barbero, S., and Cheresh, D. A. (2005) Tyrosine phosphorylation of VE-cadherin prevents binding of p120- and β-catenin and maintains the cellular mesenchymal state. *J. Biol. Chem.* **280,** 31906–31912
5. Weis, S., Cui, J., Barnes, L., and Cheresh, D. (2004) Endothelial barrier disruption by VEGF-mediated Src activity potentiates tumor cell extravasation and metastasis. *J. Cell Biol.* **167,** 223–229
6. Van Sluis, G. L., Niers, T. M., Esmon, C. T., Tigchelaar, W., Richel, D. J., Buller, H. R., Van Noorden, C. J., and Spek, C. A. (2009) Endogenous activated protein C limits cancer cell extravasation through sphingosine-1-phosphate receptor 1-mediated vascular endothelial barrier enhancement. *Blood* **114,** 1968–1973
7. Rousseau, S., Houle, F., Landry, J., and Huot, J. (1997) p38 MAP kinase activation by vascular endothelial growth factor mediates actin reorganization and cell migration in human endothelial cells. *Oncogene* **15,** 2169–2177
8. Li, Y. H., and Zhu, C. (1999) A modified Boyden chamber assay for tumor cell transendothelial migration *in vitro*. *Clin. Exp. Metastasis* **17,** 423–429
9. Heyder, C., Gloria-Maercker, E., Entschladen, F., Hatzmann, W., Niggemann, B., Zänker, K. S., and Dittmar, T. (2002) Realtime visualization of tumor cell/endothelial cell interactions during transmigration across the endothelial barrier. *J. Cancer Res. Clin. Oncol.* **128,** 533–538
10. Kedrin, D., Gligorijevic, B., Wyckoff, J., Verkhusha, V. V., Condeelis, J., Segall, J. E., and van Rheenen, J. (2008) Intravital imaging of metastatic behavior through a mammary imaging window. *Nat. Methods* **5,** 1019–1021
11. Mierke, C. T. (2011) Cancer cells regulate biomechanical properties of human microvascular endothelial cells. *J. Biol. Chem.* **286,** 40025–40037
12. Mierke, C. T., Zitterbart, D. P., Kollmannsberger, P., Raupach, C., Schlötzer-Schrehardt, U., Goecke, T. W., Behrens, J., and Fabry, B. (2008) Breakdown of the endothelial barrier function in tumor cell transmigration. *Biophys. J.* **94,** 2832–2846
13. Wittchen, E. S., Worthylake, R. A., Kelly, P., Casey, P. J., Quilliam, L. A., and Burridge, K. (2005) Rap1 GTPase inhibits leukocyte transmigration by promoting endothelial barrier function. *J. Biol. Chem.* **280,** 11675–11682
14. Haidari, M., Zhang, W., Chen, Z., Ganjehei, L., Warier, N., Vanderslice, P., and Dixon, R. (2011) Myosin light chain phosphorylation facilitates monocyte transendothelial migration by dissociating endothelial adherens junctions. *Cardiovasc. Res.* **92,** 456–465
15. Di Ciano-Oliveira, C., Lodyga, M., Fan, L., Szászi, K., Hosoya, H., Rotstein, O. D., and Kapus, A. (2005) Is myosin light-chain phosphorylation a regulatory signal for the osmotic activation of the Na^+-K^+-$2Cl^-$ cotransporter? *Am. J. Physiol. Cell Physiol.* **289,** C68–C81

16. Allingham, M. J., van Buul, J. D., and Burridge, K. (2007) ICAM-1-mediated, Src- and Pyk2-dependent vascular endothelial cadherin tyrosine phosphorylation is required for leukocyte transendothelial migration. *J. Immunol.* **179,** 4053–4064
17. Haidari, M., Zhang, W., Chen, Z., Ganjehei, L., Mortazavi, A., Warier, N., Vanderslice, P., and Dixon, R. A. (2012) Atorvastatin preserves the integrity of endothelial adherens junctions by inhibiting vascular endothelial cadherin tyrosine phosphorylation. *Exp. Cell Res.* **318,** 1673–1684
18. Frost, J. A., Xu, S., Hutchison, M. R., Marcus, S., Cobb, M. H. (1996) Actions of Rho family small G proteins and p21-activated protein kinases on mitogen-activated protein kinase family members, *Mol. Cell Biol.* **16,** 3707–3713
19. Li, W., Chong, H., Guan, K. L. (2001) Function of the Rho family GTPases in Ras-stimulated Raf activation. *J. Biol. Chem.* **276,** 34728–34737
20. Khosravi-Far, R., Solski, P. A., Clark, G. J., Kinch, M. S., Der, C. J. (1995) Activation of Rac1, RhoA, and mitogen-activated protein kinases is required for Ras transformation. *Mol. Cell Biol.* **15,** 6443–6453
21. Shen, Q., Rigor, R. R., Pivetti, C. D., Wu, M. H., Yuan, S. Y. (2010) Myosin light chain kinase in microvascular endothelial barrier function. *Cardiovasc. Res.* **87,** 272–280
22. Sun, C., Wu, M. H., Yuan, S. Y. (2011) Nonmuscle myosin light-chain kinase deficiency attenuates atherosclerosis in apolipoprotein E-deficient mice via reduced endothelial barrier dysfunction and monocyte migration. *Circulation* **124,** 48–57
23. Haidari, M., Zhang, W., Ganjehei, L., Ali, M., and Chen, Z. (2011) Inhibition of MLC phosphorylation restricts replication of influenza virus. A mechanism of action for anti-influenza agents. *PLoS One* **6,** e21444
24. Ramirez, N. E., Zhang, Z., Madamanchi, A., Boyd, K. L., O'Rear, L. D., Nashabi, A., Li, Z., Dupont, W. D., Zijlstra, A., and Zutter, M. M. The $\alpha\beta$ integrin is a metastasis suppressor in mouse models and human cancer. *J. Clin. Invest.* **121,** 226–237
25. Chan, B. M., Matsuura, N., Takada, Y., Zetter, B. R., and Hemler, M. E. (1991) *In vitro* and *in vivo* consequences of VLA-2 expression on rhabdomyosarcoma cells. *Science* **251,** 1600–1602
26. Ho, W. C., Heinemann, C., Hangan, D., Uniyal, S., Morris, V. L., and Chan, B. M. (1997) Modulation of *in vivo* migratory function of $\alpha2\beta1$ integrin in mouse liver. *Mol. Biol. Cell* **8,** 1863–1875
27. Yang, C., Zeisberg, M., Lively, J. C., Nyberg, P., Afdhal, N., and Kalluri, R. (2003) Integrin alpha1beta1 and alpha2beta1 are the key regulators of hepatocarcinoma cell invasion across the fibrotic matrix microenvironment. *Cancer Res.* **63,** 8312–8317
28. Yoshimura, K., Meckel, K. F., Laird, L. S., Chia, C. Y., Park, J. J., Olino, K. L., Tsunedomi, R., Harada, T., Iizuka, N., Hazama, S., Kato, Y., Keller, J. W., Thompson, J. M., Chang, F., Romer, L. H., Jain, A., Iacobuzio-Donahue, C., Oka, M., Pardoll, D. M., and Schulick, R. D. (2009) Integrin $\alpha2$ mediates selective metastasis to the liver. *Cancer Res.* **69,** 7320–7328
29. Wu, M., Wu, Z. F., Rosenthal, D. T., Rhee, E. M., and Merajver, S. D. Characterization of the roles of RHOC and RHOA GTPases in invasion, motility, and matrix adhesion in inflammatory and aggressive breast cancers. *Cancer* **116,** 2768–2782
30. Hall, C. L., Dai, J., van Golen, K. L., Keller, E. T., and Long, M. W. (2006) Type I collagen receptor ($\alpha2$ $\beta1$) signaling promotes the growth of human prostate cancer cells within the bone. *Cancer Res.* **66,** 8648–8654
31. Hall, C. L., Dubyk, C. W., Riesenberger, T. A., Shein, D., Keller, E. T., and van Golen, K. L. (2008) Type I collagen receptor ($\alpha2\beta1$) signaling promotes prostate cancer invasion through RhoC GTPase. *Neoplasia* **10,** 797–803
32. Lundström, A., Holmbom, J., Lindqvist, C., and Nordström, T. (1998) The role of $\alpha2$ $\beta1$ and $\alpha3$ $\beta1$ integrin receptors in the initial anchoring of MDA-MB-231 human breast cancer cells to cortical bone matrix. *Biochem. Biophys. Res. Commun.* **250,** 735–740
33. van der Pluijm, Vloedgraven, H., Papapoulos, S., Löwick, C., Grzesik, W., Kerr, J., and Robey, P. G. (1997) Attachment characteristics and involvement of integrins in adhesion of breast cancer cell lines to extracellular bone matrix components. *Lab. Invest.* **77,** 665–675
34. Lee, T. H., Avraham, H. K., Jiang, S., and Avraham, S. (2003) Vascular endothelial growth factor modulates the transendothelial migration of MDA-MB-231 breast cancer cells through regulation of brain microvascular endothelial cell permeability. *J. Biol. Chem.* **278,** 5277–5284
35. Khuon, S., Liang, L., Dettman, R. W., Sporn, P. H., Wysolmerski, R. B., and Chew, T. L. (2010) Myosin light chain kinase mediates transcellular intravasation of breast cancer cells through the underlying endothelial cells. A three-dimensional FRET study. *J. Cell Sci.* **123,** 431–440
36. Miyake, Y., Inoue, N., Nishimura, K., Kinoshita, N., Hosoya, H., Yonemura, S. (2006) Actomyosin tension is required for correct recruitment of adherens junction components and zonula occludens formation. *Exp. Cell Res.* **312,** 1637–1650
37. Bruewer, M., Hopkins, A. M., Hobert, M. E., Nusrat, A., Madara, J. L. (2004) RhoA, Rac1, and Cdc42 exert distinct effects on epithelial barrier via selective structural and biochemical modulation of junctional proteins and F-actin. *Am. J. Physiol. Cell Physiol.* **287,** C327–C335
38. Nicolson, G. L. (1982) Metastatic tumor cell attachment and invasion assay utilizing vascular endothelial cell monolayers. *J. Histochem. Cytochem.* **30,** 214–220
39. Kusama, T., Nakamori, S., Ohigashi, H., Mukai, M., Shinkai, K., Ishikawa, O., Imaoka, S., Matsumoto, Y., and Akedo, H. (1995) Enhancement of *in vitro* tumor cell transcellular migration by tumor cell-secreted endothelial cell retraction factor. *Int. J. Cancer* **63,** 112–118
40. Yu, D., Wang, S. S., Dulski, K. M., Tsai, C. M., Nicolson, G. L., and Hung, M. C. (1994) c-erbB-2/neu overexpression enhances metastatic potential of human lung cancer cells by induction of metastasis-associated properties. *Cancer Res.* **54,** 3260–3266
41. Cooper, C. R., McLean, L., Walsh, M., Taylor, J., Hayasaka, S., Bhatia, J., Pienta, K. J. (2000) Preferential adhesion of prostate cancer cells to bone is mediated by binding to bone marrow endothelial cells as compared with extracellular matrix components *in vitro*. *Clin. Cancer Res.* **6,** 4839–4847
42. Bliss, R. D., Kirby, J. A., Browell, D. A., Lennard, T. W. (1995) The role of $\beta1$ integrins in adhesion of two breast carcinoma cell lines to a model endothelium. *Clin. Exp. Metastasis* **13,** 173–183